12. EXTENDED FLUID MODEL ACCOUNTING FOR NON-LOCAL IONIZATION SOURCE TERM FOR FULL-SCALE SIMULATION OF GAS DISCHARGES

I. Rafatov, B. Yedierler, E. Eylenceoglu, E. Erden
Physics Department, Middle East Technical University, Ankara, Turkey
E. A. Bogdanov, A. A. Kudryavtsev
Saint Petersburg State University, St. Petersburg, Russia

1. Introduction

Different approaches that are used for the gas discharge modeling can by classified as fluid models, kinetic (particle) models, and their combinations known as hybrid models. Advantages of the fluids models are their relative simplicity and computational efficiency. However, these models are very approximate, mainly due to the "local field approximation", which is usually employed by fluid models to determine the transport parameters and the ionization rate [1].

The nonlocal kinetics of electrons is approximately taken into account in the "extended fluid models", in which the electrons are described in terms of fluid dynamics but their transport and kinetic coefficients are calculated as functions of the electron temperature rather than of the local electric field, through the solution of the local Boltzmann equation [2].

Exact description of electron behavior can be obtained by solving kinetic Boltzmann equation [3]. However, this approach is mathematically very complicated. Method known as PIC/MCC, which couples MC simulations for the behavior of electrons and ions to the Poisson equation for the self-consistent electric field, is also time consuming [4].

Necessity of separate treatment of different, independently behaving electron groups (i.e. non-locality of their EDF) leads to development of hybrid models, which represent a compromise between computationally effective but very approximate fluid models and accurate but time consuming particle and kinetic models [5]. Basically, two main groups of electrons are identified, which are high energetic (fast) electrons and low energetic (slow) bulk electrons. Hybrid models usually employ Monte Carlo method for fast electron dynamics, while slow plasma species are described as fluids.

In this work, we incorporated effect of fast electrons into the "extended fluid model" of glow discharge by the analytical approximation of the ionization source function [1, 6], and then integrating it into the fluid model. Comparison with the experimental data as well as with the hybrid and particle modeling results exhibits good applicability of the proposed model.

2. Fluid model

Fluid model for the gas discharge includes continuity equations for the charged and excited particles,

$$\frac{\partial n_k}{\partial t} + \nabla \cdot \boldsymbol{\Gamma}_k = S_k, \qquad (1)$$

completed with the Poisson equation for the electrostatic field,

$$\varepsilon_0 \nabla \cdot \boldsymbol{E} = \sum_k q_k n_k \,, \boldsymbol{E} = -\nabla\varphi \qquad (2)$$

Here, subscript k indicates the kth species (we will also use subscripts i, e, m and g for the ions, electrons, metastable atoms and background gas, respectively), n stands for the number density, S denotes the particle creation rate, $\boldsymbol{E}$ and φ are the electric field and potential, q is the charge, and ε_0 is the dielectric constant. $\boldsymbol{\Gamma}$ denotes the particle flux, which, with parameters μ and D denoting the mobility and diffusion coefficients, is given in the drift-diffusion approximation,

$$\boldsymbol{\Gamma}_k = sgn(q_k)\mu_k n_k \boldsymbol{E} - D_k \nabla n_k \quad (3)$$

Equations (1)–(3), with particle transport coefficients and volume source terms in the particle balance equations specified, form the traditional "simple fluid" model. Within this model,

Table 1. Elementary reactions considered in this study. Label Boltz. indicates that constant was calculated from local Boltzmann equation.

Index	*Reaction*	*Type*	*ΔE (eV)*	*Constant*
1	$e + Ar \longrightarrow e + Ar$	Elastic collision	0	Boltz.
2	$e + Ar \longrightarrow 2e + Ar^+$	Direct ionization	15.8	Boltz.
3	$e + Ar \leftrightarrow e + Ar^*$	Excitation	11.4	Boltz.
4	$e + Ar \longrightarrow e + Ar$	Excitation	13.1	Boltz.
5	$e + Ar^* \longrightarrow 2e + Ar^+$	Stepwise ionization	4.4	Boltz.
6	$2Ar^* \longrightarrow e + Ar^+ + Ar$	Penning ionization	-	6.2×10^{-10} cm^3s^{-1}
7	$Ar^* \longrightarrow h\nu + Ar$	Radiation (including trapping)	-	$1.0\times10^7 s^{-1}$

particle creation rate is determined as function of reduced electric field E/p ("local field approximation"), which, in general, is an unacceptable approximation [1]. In order to incorporate the nonlocal transport of electrons into the fluid model, electron energy equation is included in the set of "extended fluid model" equations (see, e.g., [2]),

$$\frac{\partial n_\varepsilon}{\partial t} + \nabla \cdot \boldsymbol{\Gamma}_\varepsilon = S_\varepsilon$$

where $n_\varepsilon = n_e \bar{\varepsilon}$ is the electron energy density, $\bar{\varepsilon} = 3/2\, k_B T_e$ denotes the mean electron energy, and density of the electron energy flux is

$$\boldsymbol{\Gamma}_\varepsilon = -\mu_\varepsilon n_\varepsilon \boldsymbol{E} - D_\varepsilon \nabla n_\varepsilon. \quad (4)$$

Energy transport coefficients are related to particle transport coefficients via $\mu_\varepsilon = (5/3)\mu_e$ and $D_\varepsilon = (5/3)D_e$.

Source function for the electron energy equation has a form

$$S_\varepsilon = P_{heat} + P_{elastic} + P_{inelastic},$$

where the first term describes the Joule heating (or cooling) of electrons in the electric field, $P_{heat} = -e\boldsymbol{\Gamma}_e \cdot \boldsymbol{E}$, the second term expresses the elastic losses,

$$P_{elastic} = -\frac{3}{2}\frac{m_e}{m_g}\nu_{ea} n_e k_B (T_e - T_g),$$

and the last term is the energy loss in inelastic collisions, $P_{inelastic} = \sum_j \Delta E_j R_j$. In these equations, ν_{ea} denotes the electron-atomic elastic collision frequency, m is the particle mass, background gas temperature $T_g = 300$ K, ΔE_j and R_j are the energy loss (or gain) due to inelastic collision and corresponding reaction rate.

Mobility and diffusion coefficients of heavy particles are approximated by constant parameters, which depends on background gas density, and related by the expression $D_i/\mu_i = k_B T_i/e$ with $T_i = T_g$. Electron mobility, μ_e, and diffusion, D_e, are computed from

$$\mu_e = -\frac{1}{n_e}\frac{e}{m_e}\int_0^\infty D_r \sqrt{\varepsilon}\frac{\partial}{\partial \varepsilon} f_0(\varepsilon) d\varepsilon,$$

$$D_e = -\frac{1}{n_e}\int_0^\infty D_r \sqrt{\varepsilon}\, f_0(\varepsilon) d\varepsilon,$$

where $\varepsilon = mv^2/2e$ is the electron kinetic energy (in eV units), v is the electron velocity, $D_r = 2\varepsilon/3m_e\nu_{ea}$ is the space diffusion coefficient, and $f_0(\varepsilon)$ is the EEDF obtained from the solution of the local Boltzmann

equation.

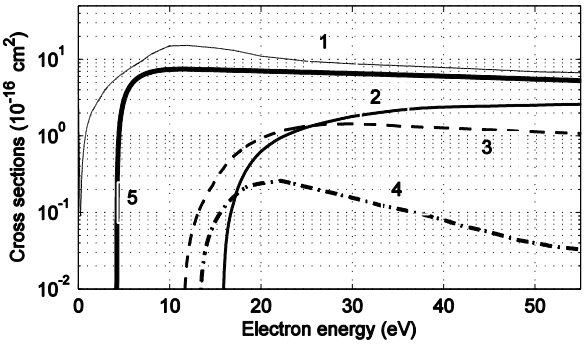

FIG. 1. Electron cross sections for (1) elastic, (2) direct ionization, (3) excitation, (4) excitation, and (5) stepwise ionization collisions in argon, used in the model. Curve labels correspond to indices of corresponding processes in Table 1.

The calculations were performed for an argon gas, and three plasma species, namely, electrons, positive ions, and metastable atoms were taken into account. The set of reactions is given in Table 1, and collision cross-sections are shown in Fig. 1.

Balance of charged particles, in the absence of recombination, is determined by the direct, stepwise, and Penning ionization processes,

$$S_e = S_i = K_2 n_0 n_e + K_5 n_m n_e + K_6 n_m^2$$

Here, K denotes the constant of the corresponding reaction, n_0 is the concentration of neutral atoms. Reaction constants are numbered according to the list of processes in Table 1. Balance of excited atoms is determined by the reactions of excitation, deexcitation, stepwise ionization, Penning ionization and radiation,

$$S_m = K_3 n_0 n_e - K'_3 n_m n_e - K_5 n_m n_e - 2K_6 n_m^2 - K_7 n_m,$$

where K_3' is the rate constant of superelastic electron collisions, which correspond to the left-directed arrow for the process 3 in Table 1. Cross-section corresponding to this process is determined by the detailed balance relationship.

For the electron-induced reactions (processes 1–5 in the Table 1), rate constants K are calculated by convolving the EEDF, obtained from the solution of the local Boltzmann kinetic equation, with the corresponding cross-sections,

$$K_R = \int_0^\infty \sigma_R(\varepsilon) v(\varepsilon) \sqrt{\varepsilon} f_0(\varepsilon) d\varepsilon.$$

3. Models with a nonlocal ionization source

We formulated the nonlocal ionization source in the way suggested in Refs. [1, 6]. The discharge gap is divided into two regions, namely, the cathode sheath region where the electric field is strong, and the plasma region, where the field is weak. These regions are separated by a point $x = d$, the sheath boundary, which is determined as a distance x from the cathode such that the equality $n_e(x) = 0.5\, n_i(x)$ holds. Since the ionization source term $S_{fast}(x)$ decays exponentially with distance from the sheath boundary, it can be approximated as

$$S_{fast}(x) \propto e^{-\alpha(x-d)/\lambda} \quad (x \geq d)$$

with a decay constant λ. Taking into account that the maximum value of the ionization source is

$$S_{fast}(x) = \Gamma_e(0) \alpha e^{\alpha d},$$

where $\Gamma_e(0)$ is the electron flux density at the cathode and α is the Townsend ionization coefficient, function S takes the form

$$S_{fast}(x) = \begin{cases} \Gamma_e(0) \alpha e^{\alpha x} & \text{for } x < d \\ \Gamma_e(0) \alpha e^{\alpha d} e^{-\frac{\alpha(x-d)}{\lambda}} & \text{for } x \geq d \end{cases} \quad (5)$$

We approximated Townsend ionization coefficient α by the estimation from Ref. [7], with the effective field $\mathcal{E}$ calculated as average field over the cathode sheath, $\mathcal{E} = \varphi(d)/d$. As a decay constant λ, we used an estimation proposed in Ref. [1],

$$\lambda = \frac{\varphi(d)/(pB) - d}{\alpha d}, \quad (6)$$

where $B = 180$ V/(cm · Torr) for an argon gas.

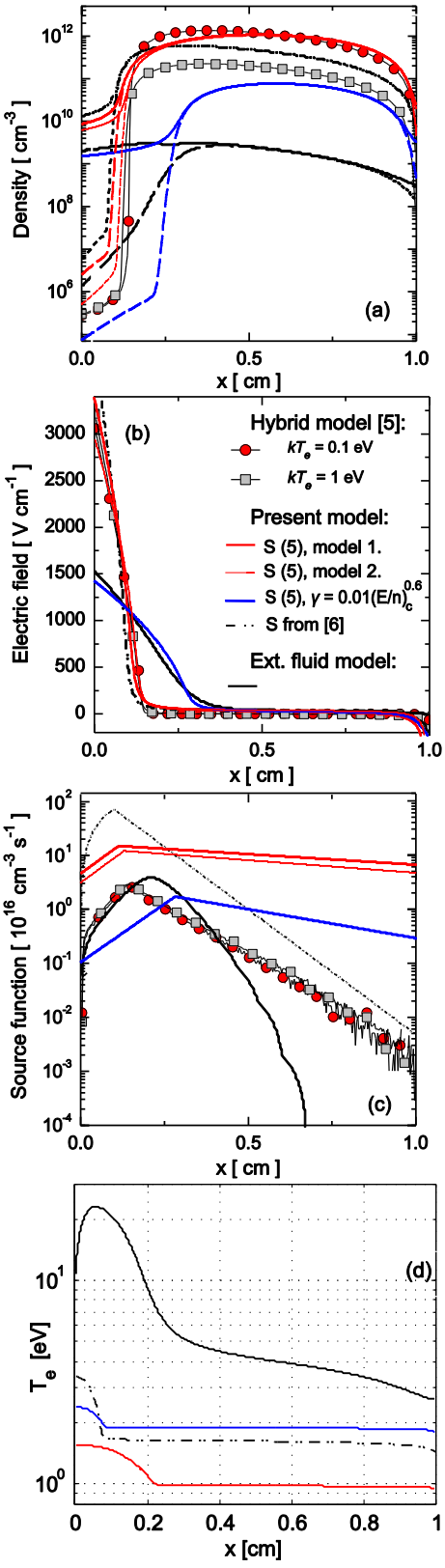

FIG. 2. Comparison with the hybrid model results from Ref. 5, for the set of conditions $p = 133$ Pa, $V = 250$ V, $L = 1$ cm, $\gamma = 0.06$. Spatial distributions of (a) electron and ion density, (b) electric field, (c) ionization source function, (d) electron temperature.

We incorporated ionization function S_{fast} defined by (5) into

1. "simple" fluid model of glow discharge, where the plasma is composed of two species only, namely, the positive ions and electrons, and the ionization source function is

$$S_e = S_i = S_{fast}$$

2. "extended" fluid model of glow discharge with,

$$S_e = S_i = S_{fast} + K_2 n_0 n_e + K_5 n_m n_e + K_6 n_m^2,$$

$$S_m = 0.5 S_{fast} + K_3 n_0 n_e - K'_3 n_m n_e - K_5 n_m n_e - 2K_6 n_m^2 - K_7 n_m.$$

In the model 1, electron mobility and diffusion, μ_e and D_e, have been taken to be constants corresponding to those of the model 2, corresponding to the temperature $T_e = 1$ eV. Heating term in the equation of electron energy balance is estimated (see Ref. [8] for details) by

$$P_{fast} = \frac{1}{2}\Delta E_3 S_{fast} \frac{\nu_{ee}}{\nu_{ee} + \delta\nu_{ea} + \nu_{df}},$$

where $\nu_{df} = \Lambda^2 / D_{ef}$, Λ is the characteristic diffusive scale, D_{ef} is the free diffusion coefficient of electrons.

4. Boundary Conditions

Boundary condition for the positive ions, metastable atoms, and electron energy density at the anode and cathode are given as follows

$$\hat{\boldsymbol{n}} \cdot \boldsymbol{\Gamma}_i = 1/4\, v_i n_i + \alpha n_i \mu_i (\hat{\boldsymbol{n}} \cdot \boldsymbol{E}),$$

$$\hat{\boldsymbol{n}} \cdot \boldsymbol{\Gamma}_m = 1/4\, v_m n_m,$$

$$\hat{\boldsymbol{n}} \cdot \boldsymbol{\Gamma}_\varepsilon = 1/3\, v_e n_\varepsilon.$$

Here, $v_j = \sqrt{8k_B T_j / \pi m_j}$ $(j = e, i, m)$ denotes the thermal velocity, the flux density $\boldsymbol{\Gamma}$ is described by the equations (3) and (4), $\hat{\boldsymbol{n}}$ is the normal unit vector pointing towards the surface, and α is a switching function (either 0 or 1) depending on positive ion

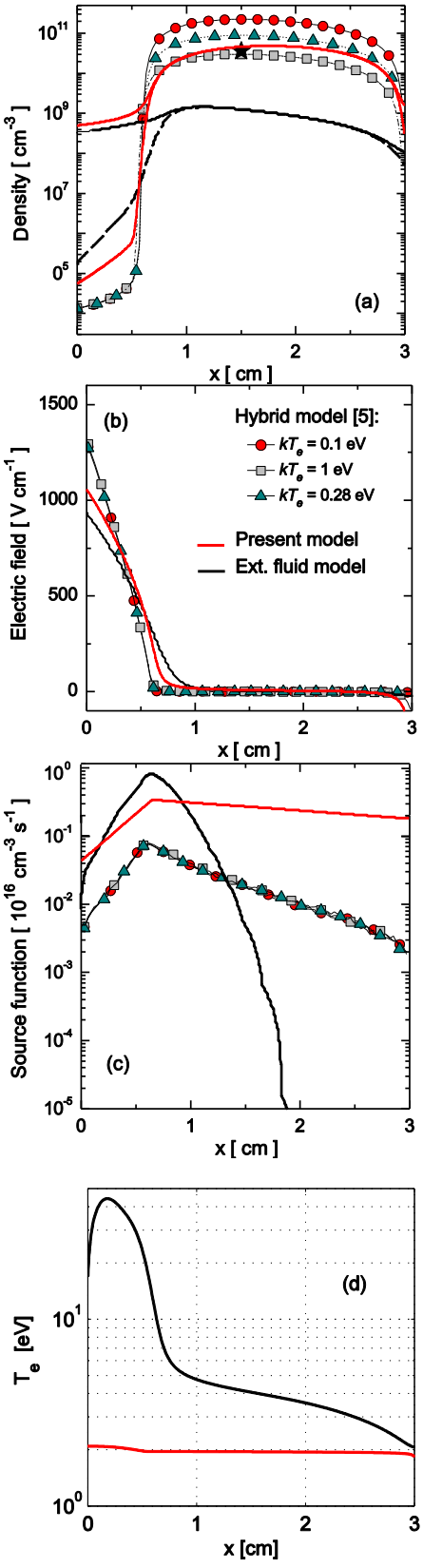

FIG. 3. Comparison with the hybrid model results from Ref. 5, for the set of conditions $p = 40$ Pa, $V = 441$ V, $L = 3$ cm, $\gamma = 0.033$. Spatial distributions of (a) electron and ion density, (b) electric field, (c) ionization source function, (d) electron temperature.

drift direction at the surface: $\alpha = 1$ if $(\hat{\boldsymbol{n}} \cdot \boldsymbol{E}) > 0$ and $\alpha = 0$ otherwise.

Boundary conditions for the electron density at the anode is

$$\hat{\boldsymbol{n}} \cdot \boldsymbol{\Gamma}_e = 1/4\, v_e n_e,$$

and at the cathode

$$\hat{\boldsymbol{n}} \cdot \boldsymbol{\Gamma}_e = 1/4\, v_e n_e - \gamma \hat{\boldsymbol{n}} \cdot \boldsymbol{\Gamma}_i,$$

where γ is the secondary electron emission coefficient.

For the electric potential, we set $\varphi = U_d$ at the anode and $\varphi = 0$ at the cathode.

5. Modelling results

In order to demonstrate the performance of the model, first we carried out test simulations for the discharge conditions from Ref. 5. Figures 2 and 3 compare spatial distributions of the discharge parameters obtained by the hybrid model from Ref. 8 with those obtained from the present model, for the two sets of conditions. The first set comprises $p = 133$ Pa, $V = 250$ V, $L = 1$ cm, $\gamma = 0.06$. For the second set, the parameters are $p = 40$ Pa, $V = 441$ V, $L = 3$ cm, $\gamma = 0.033$. Figures 2 and 3 contain (a) the distributions of the electron and ion densities, n_e and n_i (b) electric field magnitude E, (c) ionization source functions S, and (d) electron temperature, T_e. These figures illustrate also numerical results obtained by the ”extended fluid” model, and the results obtained with the ionization function from Ref. [6] integrated into the ”extended” fluid model.

As can be seen from Figs. 2 and 3, proposed model provides much better performance compared to the ”extended fluid” model. Magnitudes and shapes of the charged particle densities (panels (a)) as well as the electric field (panels (b)) are closed to those obtained from the hybrid model. Also, the electron temperature is not overestimated as in the case of the ”extended fluid” model (panels (d)).

As can be seen from Fig. 2, models

with nonlocal ionization source, derived from the ”simple” and ”extended” fluid models, practically coincide under the studied (short) discharge conditions, because the nonlocal ionization term dominates over other ionization processes involved, namely stepwise and Penning ionizations.

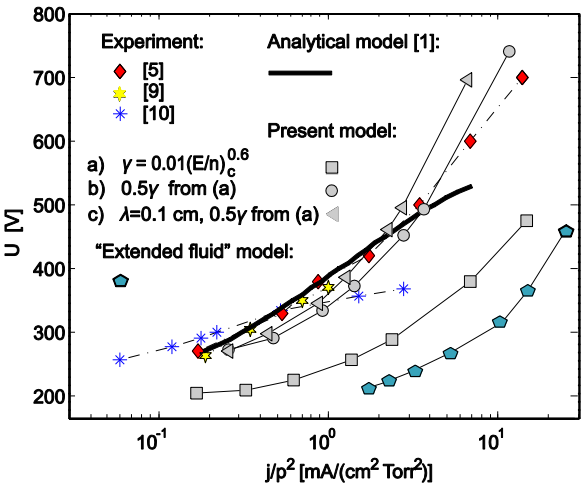

FIG. 4. Voltage as a function of the reduced current density, for $pL = 0.5$ cmTorr. Measured data are from Ref. [4, 9-10]. Present model results with different approximations for the parameters γ and λ as indicated in the legend.

As always in models for the glow discharge, secondary emission coefficient γ is one of the main sources of uncertainty. In order to demonstrate the effect of this parameter, Fig. 2 contains also numerical result obtained using the parameter γ approximated by [7]

$$\gamma = 0.01(E/n)_c^{0.6}, \qquad (7)$$

where the reduced electric field is evaluated at the cathode, and given in units of kTd (1 kTd = 10^{-20} Vcm^2). For the second reference conditions set, γ determined by (7) appears to be very close to $\gamma = 0.033$ such that the numerical results obtained with these parameters practically coincide.

Figure 4 compares measured volt-ampere characteristics (VAC) of Refs. [4, 9-10] and VAC from the semi-analytical calculations of Ref. [1] with those obtained from the present model for $pL = 0.5$ cmTorr, with parameter γ approximated by the equation (7) and one half of this γ, and with parameter λ determined by (6) and by constant $\lambda = 0.1$ cm. It is seen that results of the proposed model are close to those obtained from the measurements and it provides much better performance compared to the ”extended fluid” model.

Conclusions

We developed and tested a simple hybrid model for a glow discharge, which incorporates nonlocal ionization by fast electrons into the fluid framework, and thereby overcomes the fundamental shortcomings of the fluid model. At the same time, proposed model is computationally much more efficient compared to the models involving Monte Carlo simulations.

Calculations have been performed for an argon gas. Comparison with the experimental data as well as hybrid (particle) and fluid modelling results exhibits good applicability of the proposed model.

ACKNOWLEDGMENTS

The work was supported by the joint research grant from the Scientific and Technical Research Council of Turkey (TUBITAK) 210T072 and Russian Foundation for Basic Research (RFBR).

[1] A. A. Kudryavtsev, A. V. Morin, and L. D. Tsendin, Tech. Phys. **53**, 1029 (2008).

[2] J.P. Boeuf and L. C. Pitchford, Phys. Rev. E **51**, 1376 (1995).

[3] R. E. Robson, R. D. White, and Z. Lj. Petrovi´c, Rev. Mod. Phys. **77**, 1303 (2005).

[4] Z. Donko, P. Hartmann, and K. Kutasi, Plasma Sources Sci. Technol. **15**, 178 (2006).

[5] A. Derzsi, A. Hartmann, I. Korolov, J. Karacsony, G. Bano, and Z. Donko, J. Phys. D: Appl. Phys. **42**, 225204 (2009).

[6] I. Peres, N. Ouadoudi, L. C. Pitchford, and J.P. Boeuf, J. Appl. Phys **72**, 4533 (1992).

[7] A. V. Phelps, Z. Lj. Petrovic, Plasma Sources Sci. Technol. **8**, R21 (1999).

[8] N. V. Bedenkov, A. A. Kudryavtsev, V. A. Romanenko, S. A. Solodkiy, Physica Scripta **53**, 490 (1996).

[9] K. Rozsa, A. Gallagher, and Z. Donk´o, Phys. Rev. E **52**, 913 (1995).

[10] I. Stefanovic and Z. Lj. Petrovic, Japan. J. Appl. Phys. **36**, 4728 (1997).